Read Channel Modeling for Detection in Two-Dimensional Magnetic Recording Systems

Anantha Raman Krishnan, Rathnakumar Radhakrishnan, *Member, IEEE* and Bane Vasic, *Senior Member, IEEE*

***Abstract*—In this paper, we describe a read channel model for detector design for two dimensional magnetic recording (TDMR) system, a novel strategy for recording at upto 10 Tb/in^2. We describe a scheme for (1) modeling of the recording medium, (2) modeling of the write/readback process, and (3) an experimental method for the characterization of noise in the TDMR channel, occurring due to irregularities in the bit-boundaries in the recording medium, that can be used for detection purposes.**

I. Introduction

Even with the advent of recording systems with storage density exceeding 250 Gb/in.^{2}, research has already begun on the development of next-generation magnetic recording systems capable of achieving 10 Tb/in^2. The technologies being investigated in this regard are Heat-Assisted Magnetic Recording (HAMR) [1], Bit-Patterned Media (BPM) [2] and Two-Dimensional Magnetic Recording (TDMR) [3]. HAMR and BPM rely on the use of novel recording media to achieve high recording density. In contrast, TDMR relies on conventional media for storage while taking a more aggressive approach to writing and reading. More specifically, a system which reliably stores user-bit in very few grains (possibly 1 grain/bit) is envisioned.

From a signal processing perspctive, TDMR paradigm for storage presents a number of challenges such as read channel modeling, detection in the presence of severe two-dimensional (2D) ISI, code design for the channel, *etc*. The most critical of these is the modeling of the read channel for detector design. In TDMR, since the area allocated for the storage of a bit (bit-area) is comparable to the area of grains, the boundaries of bit-area are extremely irregular. In this case, MicroTrack models [4] are not accurate. Two models of recording medium were proposed in [5]. The first model simulates the recording medium as a collection of grains which could take up one of a finite number of predetermined shapes. The second model uses the variance in grain shapes and sizes to determine a realistic representation of the medium and then uses sophisticated rules to simulate the writing process. The first model, although lacking accuracy, is well-suited for capacity calculation. The second model is more accurate. However, it is very complex and hence not well-suited for studying error rate performance for various detection and coding schemes. Hence, the need for a good read channel model that provides a good trade-off between accuracy and complexity is necessary. Another challenge lies in the detection of channel bits in the presence of noise. In contrast to conventional recording systems, the primary source of noise in TDMR comes from the irregular boundaries of grains and the lack of knowledge of these boundaries during the readback process (often this is low enough to bring the signal to noise ratio (SNR) to below 0 dB[3]). Accurate modeling of this noise is also important.

In this paper, we present a read channel model for detector design based on Voronoi tilings that achieves a good trade-off between complexity and accuracy. This model can be used to characterize the noise experimentally, and to develop detection algorithms for TDMR. The rest of the paper is organized as follows: Section II describes a read channel model for TDMR. Section III describes the characterization of noise. In Section IV, we summarize our work and discuss use of this noise model in some conventional detection schemes and possible future work.

A. R. Krishnan, R. Radhakrishnan and B. Vasic are with the Department of Electrical and Computer Engineering, The University of Arizona, Tucson, AZ, 85721 USA e-mail: {ananthak, rathna, vasic}@ece.arizona.edu.

II. Read Channel Model

A. Modeling the recording medium

Before we describe the model for the recording medium, for the sake of completeness, we give a brief introduction to Voronoi tiling of planes. Let $\mathcal{S}$ be a set of points on the Euclidean plane. Then, the Voronoi region of the point $s \in \mathcal{S}$, $\mathcal{A}_s$, is the set of all points in the plane closer to s than to any other point belonging to $\mathcal{S}$. Fig. 1 shows an example of a Voronoi tiling. The figure shows the regions of points 1 through 6. For example, the region $\mathcal{A}_1$ contains the points which are closer to 1 than to points 2-6. All the points on the boundary are equi-distant from their two closest points.

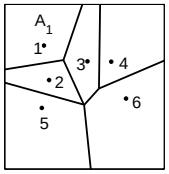

Fig. 1. Voronoi tiling of plane.

We seek to model the recording medium as a Voronoi tiling of a plane with the regions of points in the plane representing its constituent grains. First, consider the "ideal" medium (from the perspective of detector). In such a medium, all the grains would be of equal size and would be regularly spaced. Hence, it can be visualized as the Voronoi tiling of equi-spaced points in a plane. Note that depending on the orientation of the equi-spaced points relative to each other, three possible Voronoi tilings can occur, namely, the tiling of the plane with triangles, squares and regular hexagons. We choose the

orientation corresponding to the tiling of a plane with squares, namely, points on a square lattice, as it represents a faithful model for the linear fashion of reading/writing proposed in TDMR [3].

Let S be a set of points in the square lattice. Then, the regions of points belonging to S is our model of grains in the ideal medium. We refer to the points in S as *cell-centers* and to their regions as *cells*. Fig. 2(a) shows an example of a plane of dimension 3 cells$\times$3 cells with the cell-centers marked as '$*$'. The cell-boundaries are marked by dashed lines.

The randomness in the shape and position of grains is modeled by shifting the grain-centers randomly from the cell-centers. The recording medium can then be visualized as the Voronoi tiling of the shifted grain-centers with their regions representing the grains. Fig. 2(b) shows an instance of recording medium of size 3 cells$\times$3 cells (a medium of dimension m cells$\times n$ cells will henceforth be referred to as an $m \times n$ medium). The cell-centers are marked as '$*$' and the shifted grain centers are marked as '$\bullet$'. The cell-boundaries are marked by dashed lines and the grain-boundaries are marked by solid lines.

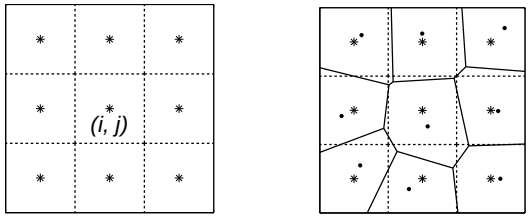

(a) (b)

Fig. 2. Modeling of recording medium: (a) an example of ideal medium; and (b) an example of a practical medium.

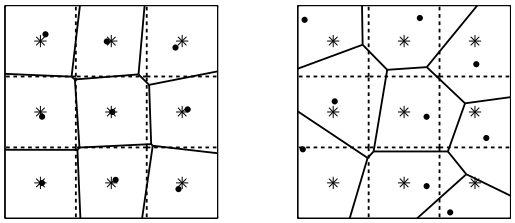

(a) (b)

Fig. 3. Choice of distribution of shift of grain-center: (a) An example of a distribution with small average shift; and (b) an example of a distribution with large average shift.

In modeling the medium this way, we assume that the shift of the grain-centers from their ideal positions follows some known probability distribution and that the shifted grain-centers are always within their corresponding cells. Note that the choice of the distribution affects the degree of variation in the grain sizes, positions and their boundaries. Fig. 3 illustrates the effect of choice of distribution on these parameters with two examples. The medium shown in Fig. 3(a) has a smaller average shift in grain-centers than the one shown in Fig. 3(b). The boundaries of the ideal medium are denoted by the dotted line. It is readily seen that the medium shown in Fig. 3(a) is "closer" to the ideal medium than the medium shown in Fig. 3(b). Without prior knowledge, it is reasonable to assume that the shifts are uniformly distributed within the area of the cell. Note that this model can be further generalized by allowing shifts to straddle cell-boundaries. This will result in higher variance in grain area, and less regular tilings with lower long-range correlations.

B. Modeling the Write and the Readback Process

Since the read/write mechanism does not have *a priori* knowledge of the irregular grain pattern of the medium, it simply attempts to write at the cell-centers, thus giving rise to many errors. This process is appropriately mimicked for the medium represented as regions. In order to model the write process we use the following rule: The write-head writes at the center of each cell. The grain whose center is within the cell is then appropriately magnetized. An example of the difference between the magnetization of an ideal medium and an actual medium as a result of this writing process is shown in Fig. 4. Figs. 4(a) and 4(b) show the magnetization of an ideal and the actual 14×14 medium, respectively. The grains with magnetizatoin $+1$ are coloured black and the ones with magnetization -1 are coloured white.

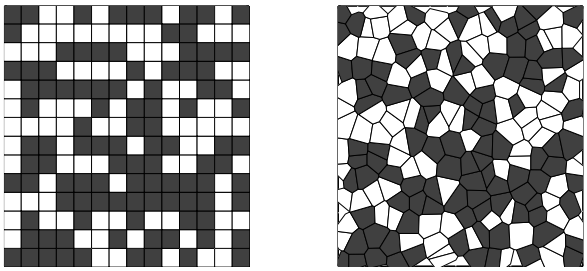

(a) (b)

Fig. 4. Writing on the recording medium: (a) The resultant magnetization of an ideal medium; and (b) The resultant magnetization of a conventional medium.

The readback signal can be obtained easily by convolving the magnetization of the medium with the response of the read-head and then sampling them at cell-centers. The response of the read-head can be obtained by using the method of Wilton and McKirdy [6], [3]. We assume the response to be a truncated 2D Gaussian pulse of unit energy with half-maximum of 1 cell-width and a span of 3 cells in both dimensions. The profile of the head-response is shown in Fig. 5.

III. Characterization of Noise

In contrast to conventional recording systems, electronic noise in TDMR is negligible when compared to noise arising from the inability of the read-mechanism to distinguish the bit/grain boundaries. Hence, it is necessary to first characterize this noise.

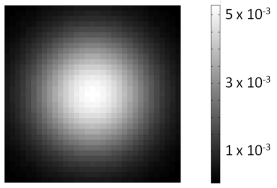

Fig. 5. Response of read-head.

In an ideal medium, as a result of the local nature of the read-head response, the readback signal at the center of any cell (i,j) depends only on the polarity of the grains in the 3×3 neighbourhood of the $(i,j)^{th}$ cell, $\mathcal{N}_{i,j}$ (as depicted in Fig. 2(a)). However, in practice, there is a change in the readback signal due to the shift in the grain-boundaries. We consider this change in the output as *noise*. This noise depends not only on the regions of grains in $\mathcal{N}_{i,j}$, but also on their polarity, as will be discussed later. As a result, this noise is correlated in both the down-track and the cross-track directions.

Let $\mathbf{X} = \{x_{1,1}, x_{1,2}, \ldots, x_{n,n}\} \in \{-1,+1\}^{n^2}$ be the input magnetization in a medium of size $n \times n$ cells and let $\mathbf{Y} = \{y_{1,1}, y_{1,2}, \ldots, y_{n,n}\}$ be the received signal at their corresponding cell-centers. Ideally, characterization of noise in TDMR entails the estimation of the conditional probability density function (pdf) $p(\mathbf{Y}|\mathbf{X})$. However, the correlated nature of this noise makes it difficult to estimate this quantity. Instead, by assuming that the noise samples are independent of each other, we attempt to estimate a numerically tractable quantity, namely, $p(y_{i,j}|\mathbf{X})$. Now, the conditional pdf can be expressed as:

$$p\left(\mathbf{Y}|\mathbf{X}\right) = \prod_{i}^{n}\prod_{j}^{n} p\left(y_{i,j}|\mathbf{X}\right) = \prod_{i}^{n}\prod_{j}^{n} p\left(y_{i,j}|\mathcal{N}_{i,j}\right). \quad (1)$$

The second part of Eqn. 1 arises from our observation that the output $y_{i,j}$ depends only on the data and region in the neighbourhood $\mathcal{N}_{i,j}$.

The densities $p\left(y_{i,j}|\mathcal{N}_{i,j}\right)$ are estimated experimentally by means of histograms. For a given 3×3 binary input, several instances of 3×3 medium are generated onto which the binary input is written. By calculating the corresponding readback output, $y_{i,j}$, an estimate of $p\left(y_{i,j}|\mathcal{N}_{i,j}\right)$ is obtained.

The number of possible 3×3 binary inputs is $2^9 = 512$, which implies that 512 conditional pdfs are required . However, symmetry in the read-head response along the down-track and cross-track directions can be exploited to reduce the number of conditional pdfs required. To see this, consider the $(i,j)^{th}$ cell in an ideal medium. It shares an edge with four cells (edge-sharing neighbours) and a vertex with four other cells (vertex-sharing neighbours). The $(i,j)^{th}$ cell along with these eight cells form its neighbourhood $\mathcal{N}_{i,j}$. The output $y_{i,j}$ depends only on (1) the polarity of the $(i,j)^{th}$ cell, (2) the number of edge-sharing neighbours with polarity $+1$, and (3) the number of vertex-sharing neighbours with polarity $+1$. This is because the symmetry in the read-head response ensures that the contribution of an edge(vertex)-sharing neighbour to the output $y_{i,j}$ is independent of its position relative to the $(i,j)^{th}$ cell. As an example, consider the output at the center of two 3×3 inputs (read row-wise),namely, [(-1 +1 -1),(-1 -1 +1),(-1 -1 -1)] and [(+1 -1 +1),(-1 -1 -1),(-1 -1 -1)]. The inputs are shown in Figs. 6(a) and 6(b), respectively. Cells with magnetization $+1$ are coloured black and ones with magnetization -1 are coloured white. The outputs corresponding to Figs. 6(a) and 6(b) are equal because they have the same polarity in the center cell and have equal number of edge- and vertex-sharing neighbours with polarity $+1$. Similarly, the outputs corresponding to Figs. 6(c) and 6(d) are equal. We say that all 3×3 neighbourhoods with the same polarity of center cell and same number of edge- and vertex-sharing neighbours with polarity $+1$ belong to the same *configuration class*.

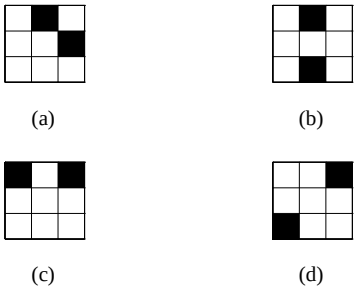

Fig. 6. Symmetry in the ideal medium: The final output at the center-cell in Figs. (a) and (b) are equal. The output at the center-cell in Figs. (c) and (d) are equal.

For a given instance of a non-ideal recording medium, the output corresponding to each 3×3 binary input differs, even if they belong to the same configuration class, because of the asymmetric grain boundaries. However, since the grain centers are independent and uniformly distributed, the conditional pdfs of the 3×3 binary inputs belonging to the same configuration are approximately same, as has been verified experimentally.

It is easy to see that there are only 50 such unique configurations. Consequently, the number of conditional pdfs required to characterize noise in TDMR is reduced to 50 from 512. Fig. 7 shows the histograms obtained experimentally. In the figure, C, E and V represent the polarity of the center cell, the number of edge neighbours with polarity $+1$, and the number of vertex-neighbours with polarity $+1$, respectively (The histogram for $C = +1$ can be obtained by noting that the histograms of $(C,E,V) = (-1,e,v)$ and $(C,E,V) = (+1,4-e,4-v)$ are symmetric about the y-axis).

The preceding discussion suggests that the conditional pdfs of the output depend only on the configuration to which the 3×3 input belongs. However, we wish to emphasize that the pdfs vary *slightly* for various 3×3 inputs belonging to the same configuration. This is due to the invariance of the output with respect to change in the boundaries between grains that are of the same polarity. For example, consider the two 3×3 inputs (read row-wise), [(-1 -1 +1),(+1 +1 +1),(+1 -1 +1)] and [(+1 -1 +1),(+1 +1 -1),(-1 +1 +1)]. Both inputs belong to the same configuration, but as Fig. 8 shows, the pdf corresponding to the first input has a smaller variance than the pdf corresponding to the second input. This is because of the fact that in the first

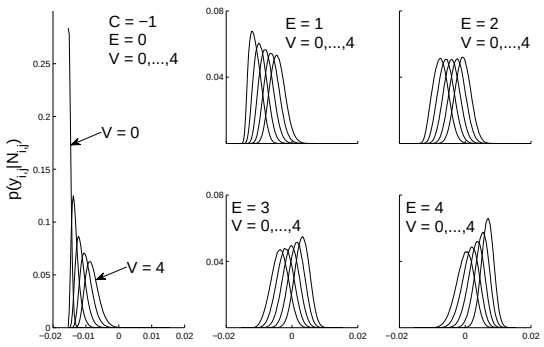

Fig. 7. Conditional pdf's of readback signal for center-bit $C = -1$ and various values of E and V.

input, two grains with polarity -1 are adjacent to each other. Consequently, the irregularity in the boundary shared by these two grains does not introduce any noise to the output of the center cell. The lack of such boundaries in the second input leads to a wider profile of the pdf. However, we consider this change in the pdfs small enough to be neglected. A corollary of this observation is that the pdfs corresponding to the all-zero and all-one inputs will be very narrow as confirmed by Fig. 7.

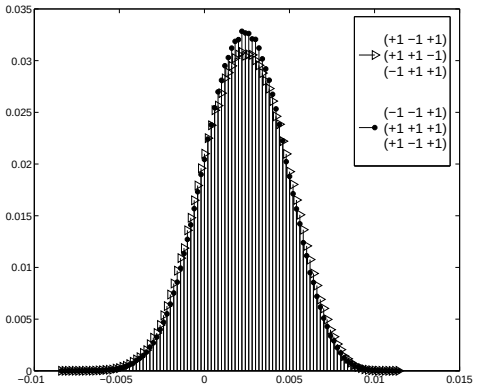

Fig. 8. Histograms of two different 3×3 input patterns.

Detection: The noise model we developed lends itself easily for use in maximum likelihood (ML) and maximum *a posteriori* (MAP) detection schemes that operate on the trellis of the TDMR channel. To analyze the performance of conventional detection schemes under our noise model, we simulated the three-track Viterbi algorithm (3TVA) [7] and the decision feedback Viterbi algorithm (DFVA) [8], two well-known sub-optimal multi-track detectors, which uses our noise model. Our simulation results show that the bit-error rate (BER) of about 15% is achieved by using these detectors. We also simulated the polarity detector which simply makes a decision based on the polarity of the output. This yielded a BER of 31%. The high BER is a consequence of the assumption that the noise samples are independent (Eqn. 1) and the large overlap among the output conditional pdfs (Fig. 7).

IV. Summary and Discussion

In this paper, we developed a read channel model for TDMR systems from the perspective of detector design that achieves a good trade-off between complexity and accuracy. We also developed an experiment-based approach to characterize the primary source of noise that arises from irregular grain boundaries. Our studies highlight the intricate relationship of the noise distribution with not only on the grain shapes, but also on the input data pattern.

The high BER obtained by using our noise model in various multi-track detection schemes yield high BER. This is due to the assumption of independence between noise samples and the large overlap among the output conditional pdfs. Our results indicate that in order to reduce the BER, we need to explore the possibility of use of constrained codes, which attempts to separate the output conditional pdfs, or novel detection schemes that account for correlation in noise.

V. Acknowledgment

This work is funded by INSIC-EHDR and NSF under grant IHSC-0725405.

References

[1] R. E. Rottmayer *et al.*, "Heat-assisted magnetic recording," *IEEE Trans. Magn.*, vol. 42, no. 10, pp. 2417–2421, Oct. 2006.
[2] B. Terris *et al.*, "Patterned media for future magnetic data storage," *Microsystem Technologies*, vol. 13, no. 2, pp. 189–196, Nov. 2006.
[3] R. Wood, M. Williams, A. Kavcic, and J. Miles, "The feasibility of magnetic recording at 10 terabits per square inch on conventional media," in *Proc. of The Magnetic Recording Conference*, Jul. 2008.
[4] J. Caroselli and J. K. Wolf, "Applications of a new simulation model for media noise limited magnetic recording channels," *IEEE Trans. Magn.*, vol. 32, no. 5, pp. 3917–3919, Sept. 1996.
[5] R. Wood, "The feasibility of magnetic recording at 1terabit per square inch," *IEEE Trans. Magn.*, vol. 36, pp. 36–42, Jan. 2000.
[6] D. T. Wilton *et al.*, "Approximate three-dimensional head fields for perpendicular magnetic recording," *IEEE Trans. Magn.*, vol. 40, no. 1, pp. 148–156, Jan 2004.
[7] B. G. Roh, S. U. Lee, J. Moon, and Y. Chen, "Single-head/single-track detection in interfering tracks," *IEEE Trans. Magn.*, vol. 38, no. 4, Jul. 2002.
[8] J. F. Heanue, K. Gurkan, and L. Hesselink, "Signal detection for page-access optical memories with intersymbol interference," *Applied Optics*, vol. 35, no. 14, May 1996.